Synchronization in starlike networks of phase oscillators

Xu, Can; Gao, Jian; Boccaletti, Stefano; Zheng, Zhigang; Guan, Shuguang

Published in:
Physical Review E

DOI:
10.1103/PhysRevE.100.012212

Publication date:
2019

Synchronization in starlike networks of phase oscillators

Can Xu,[1] Jian Gao,[2] Stefano Boccaletti,[3,4] Zhigang Zheng,[1,*] and Shuguang Guan[5,†]

[1]*Institute of Systems Science and College of Information Science and Engineering, Huaqiao University, Xiamen 361021, China*

[2]*Bernoulli Institute for Mathematics, Computer Science, and Artificial Intelligence, University of Groningen, P.O. Box 407, 9700 AK, Groningen, The Netherlands*

[3]*CNR–Institute of Complex Systems, Via Madonna del Piano, 10, 50019 Sesto Fiorentino, Florence, Italy*

[4]*Unmanned Systems Research Institute, Northwestern Polytechnical University, Xi'an 710072, China*

[5]*Department of Physics, East China Normal University, Shanghai 200241, China*

(Received 28 March 2019; published 23 July 2019)

We fully describe the mechanisms underlying synchronization in starlike networks of phase oscillators. In particular, the routes to synchronization and the critical points for the associated phase transitions are determined analytically. In contrast to the classical Kuramoto theory, we unveil that relaxation rates to each equilibrium state indeed exist and remain invariant under three levels of descriptions corresponding to different geometric implications. The special symmetry in the coupling determines a quasi-Hamiltonian property, which is further unveiled on the basis of singular perturbation theory. Since starlike coupling configurations constitute the building blocks of technological and biological real world networks, our paper paves the way towards the understanding of the functioning of such real world systems in many practical situations.

DOI: 10.1103/PhysRevE.100.012212

I. INTRODUCTION

Synchronization of interacting units is a ubiquitous self-organized collective behavior [1]. The study of synchronization covers indeed a series of subjects from the areas of physics, chemistry, bioecology, engineering, and social systems [2]. A few examples are power grids [3], electrochemical [4] and spin-torque oscillators [5], neurons in the brain [6], circadian rhythms of plants and animals [7], and pedestrians on footbridges [8]. Kuramoto-like models have long served as the main prototypes for the study of synchronization [9]. In its classical version [10], an ensemble of globally coupled phase oscillators (each one rotating with a specific rhythm) experiences a second-order phase transition at a critical point when the coupling strength is large enough to compensate for the heterogeneity in the natural frequencies. As Kuramoto's scenario is typically illustrative, an increasing number of studies have originated from such a model in order to address synchronization-specific problems both theoretically and practically [11,12].

Of particular importance is the case of networked oscillators arranged in a starlike coupling configuration. Despite their topological simplicity, starlike networks (SLNs) are extremely relevant in real world systems. For instance, almost all biological and technological real world networks exhibit degree-degree correlation features which are markedly disassortative at both global and local scales [12–14], and therefore SLNs constitute the building blocks (or the main motifs) of such networks, where leading hubs interact with surrounding leaves in order to facilitate transfer and feedback processes of information or energy [15–21]. Moreover, starlike coupling structures play a direct and essential role in many other systems, including Josephson junction arrays [22], communication and social networks, and the hierarchical organization underlying cognitive functions in mammals [23]. It is therefore rather surprising that synchronous behavior in SLNs has remained so far an almost open subject for studies.

In this paper, we give a full analysis of synchronization in SLNs of phase oscillators. To this end, we will refer to a Kuramoto-Sakaguchi model, and focus on the formation mechanisms of (and the transition roots to) synchronization, as well as comprehensively describe the dynamical features of several states induced by the special coupling scheme. In particular, we will reveal that the convergence indices characterizing the relaxation times of the dynamics to each steady state are fundamental parameters of the system and remain invariant under three levels of descriptions corresponding to different geometric implications. Moreover, we will show that the phase shift is another key parameter determining the emergence (at low values of the coupling strength) of an in-phase and a splay state. The special star symmetry yields a quasi-Hamiltonian property, which is, however, partly destroyed by the phase shift that induces the formation of a splay state in a marginal region characterized by a particular eigenspectrum structure.

II. STATIONARY SOLUTIONS AND THEIR STABILITY

Our paper starts by considering N phase oscillators obeying

$$\dot{\theta}_i = \omega_i + F(\theta_i) + \frac{1}{N}\sum_{j=1}^{N} H(\theta_j), \quad i = 1, \ldots, N. \tag{1}$$

*zgzheng@hqu.edu.cn
†sguan@phy.ecnu.edu.cn

Here, the dot stands for the temporal derivative, ω_i is the natural frequency of the ith oscillator, θ_i is its instantaneous phase, $F(\theta)$ and $H(\theta)$ are smooth 2π-periodic functions, and the interactions are here seen as an effective external driving force. As our major focus is to investigate synchronization in star networks, we set (without lack of generality) $\omega_i \equiv \omega$, $F(\theta) = -\lambda \sin(\theta - \alpha)$, and $H(\theta) = -\lambda \sin(\theta + \alpha)$, where ω is the inherent frequency of the system, $\lambda > 0$ stands for the coupling strength, and $\alpha \in (-\pi/2, \pi/2)$ denotes a phase shift involved in the coupling. The model becomes

$$\dot{\theta}_i = \omega - \lambda \sin(\theta_i - \alpha) - \frac{\lambda}{N} \sum_{j=1}^{N} \sin(\theta_j + \alpha). \tag{2}$$

Equation (2) describes a set of Kuramoto-Sakaguchi oscillators in a star network with the assumption of frequency-weighted correlations [24–28]. Since the Kuramoto-like model in the star network with frequency-degree correlation is given by

$$\dot{\varphi}_h = \omega_h + \frac{\lambda}{N} \sum_{i=1}^{N} \sin(\varphi_i - \varphi_h - \alpha), \tag{3}$$

$$\dot{\varphi}_i = \omega_l + \lambda \sin(\varphi_h - \varphi_i - \alpha), \tag{4}$$

where φ_h and ω_h are the phase and natural frequency of the hub node, respectively, φ_i and ω_l are the phase and natural frequency (identical) of the ith leaf node, respectively, and N is the number of leaves. Introducing the phase difference $\theta_i = \varphi_h - \varphi_i$, and $\omega = \omega_h - \omega_l$, Eq. (2) is recovered. Alternatively, it also represents globally coupled identical Josephson junction arrays [29,30].

The most special fixed point of Eq. (2) is $\dot{\theta}_i = 0$, and $\theta_i \equiv \theta_j$, $\forall i, j$, which corresponds to a completely synchronous manifold, termed here as a spatially homogenous fixed point (HFP) [31]. Once the system converges to the manifold, HFP satisfies $\sin\theta_0 = \omega/(2\lambda\cos\alpha)$, which implies in its turn the condition $\lambda \geqslant \omega/(2\cos\alpha)$ for synchronization. Performing small perturbations away from the synchronous manifold $[\theta_i(t) = \theta_0 + \delta\theta_i(t)]$ and omitting higher-order terms, the linearized equations for the evolution of $\delta\theta_i(t)$ are

$$\delta\dot{\theta}_i(t) = \mathbf{J}(\theta_0)\delta\theta_i, \tag{5}$$

where $\mathbf{J}$ is the Jacobian matrix calculated at HFP. According to rank-1 perturbation theory [see Appendix A], the first eigenvalue [$(N-1)$-fold degenerate] of $\mathbf{J}$ is $\delta_1 = -\lambda\cos(\theta_0 - \alpha)$, and the second (single degenerate) is $\delta_2 = -2\lambda\cos\theta_0\cos\alpha$.

As $\mathbf{J}$ is diagonalizable, the algebraic multiplicity must be equal to the geometric multiplicity of each eigenvalue: the elements of the eigenvector $\mathbf{V}_1$ (corresponding to δ_1) satisfy $\sum_{j=1}^{N}\delta\theta_j = 0$ (and such a constraint indicates that the corresponding eigenspace has $N-1$ dimensions), while the elements of δ_2's eigenvector $\mathbf{V}_2$ obey $\delta\theta_i \equiv \delta\theta_j$, $\forall i, j$ (i.e., the corresponding eigenspace is one dimensional). Now, $\mathbf{V}_2$ corresponds to a perturbation direction along the synchronization manifold, and $\mathbf{V}_1$ is instead contained in a space orthogonal to $\mathbf{V}_2$ (i.e., in the transverse space of the synchronization manifold).

When $\delta_1 < 0$ and $\delta_2 < 0$ the stable regime for HFP (see Fig. 1) corresponds to $\lambda > \omega/(2\cos^2\alpha)$ for $\alpha \in (-\pi/2, 0)$, and $\lambda > \omega/(2\cos\alpha)$ for $\alpha \in [0, \pi/2)$. Together with HFP, we emphasize here that other fixed points (phase-locked states) may exist, but they can never occur spontaneously due to the symmetry of the system. The rigorous proof of the instability of all other phase-locked states is given in Appendix B (for the particular case of $\alpha = 0$).

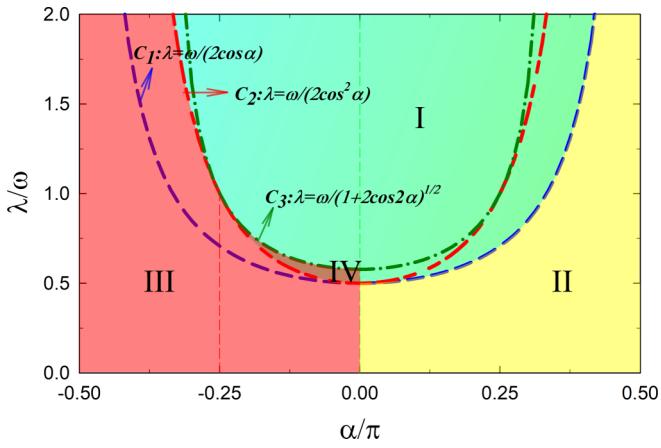

FIG. 1. Phase diagram of Eq. (2) in the space formed by the rescaled parameters α/π and λ/ω. Curves $C_{1,2,3}$ represent the existence and stability boundaries of each steady state, respectively. The green region I denotes the area where HFP is stable, and the yellow region II is the area where HLC is stable. Furthermore, the red region III represents the area where the splay state is stable, and the brown (half-moon) region IV stands for the area where there is coexistence of both the stable HFP and stable splay state. Regions III and IV together form what is called the marginal region.

The system exhibits also a periodic behavior, namely, a homogenous limit cycle (HLC) where all oscillators are in phase, and Eq. (2) converges to a one-dimensional invariant torus $\dot{\theta}(t) = \omega - 2\lambda\cos\alpha\sin\theta(t)$. Such a state can never coexist with HFP. Performing perturbations to HLC, one ends up with an orbit equation analogous to Eq. (5), with $\mathbf{J}$, which is, however, time dependent, and with $J(t)_{ij} = -\lambda\cos[\theta(t) - \alpha]\delta_{ij} - \frac{\lambda}{N}\cos[\theta(t) + \alpha]$. The solution for the perturbation vector $\mathbf{V}(t)$ is $\mathbf{V}(t) = \widehat{T}\exp\{\int_0^t dt' J[\theta(t')]\}\mathbf{V}_0$, where $\widehat{T}$ is a time-order operator and $\mathbf{V}_0$ is the initial condition. If the stationary state is a T_p-periodic limit cycle, two criteria for its stability ($I_k < 0$, $k = 1, 2$) can be obtained within the framework of the Floquet theorem (all details are contained in Appendix C), which yield $I_k = \int_0^{T_p} dt\,\delta_k(t)$. Now, I_2 is the average convergence index of the perturbation to the limit cycle which is equal to zero, and $I_1 \propto -\tan\alpha$. For $\alpha > 0$ a phase shift occurs, which can be interpreted as a dissipative factor making HLC attractive (so that all oscillators converge to a single cluster), while for $\alpha < 0$ a repulsive effect makes HLC unstable (in spite of the fact that the sign of α does not change its role as a parameter in the one-dimensional invariant torus).

Now, Eq. (2) is invariant under index transformation, and therefore all phases are dynamically equivalent. In other words, this special symmetry ensures that the oscillators can never *pass through* each other, and shows a phase order described by $\theta_N(t) \leqslant \theta_{N-1}(t) \leqslant \cdots \leqslant \theta_1(t) \leqslant \theta_N(t) + 2\pi$. Such an order defines a *canonical invariant region* in the phase space [32]. In particular, the boundary of the canonical region

corresponds to a one-dimensional manifold (HLC) containing a fixed point (HFP). In addition, the canonical region also includes a *splay* state which satisfies $\theta_i(t) = \theta(t + iT/N)$, T being a common period of phases. The splay state is induced (as a special coherent behavior) by asymmetries in the coupling scheme that may always appear in practical implementations of globally coupled oscillators' systems [29,30,33–35].

To better clarify the dynamical properties of the splay state (and elucidate its stability) we concentrate on the thermodynamic limit $N \to \infty$. There, the discrete index i in Eq. (2) is replaced by a continuous variable θ, and a probability density function $\rho(\theta, t)$ is introduced in order to describe the statistic features of the system. In this representation, the splay state corresponds to a steady distribution. Obviously, $\rho(\theta, t)$ follows a suitable normalization condition and is positive and 2π periodic with respect to θ. Therefore, the dynamical evolution of one body in Eq. (2) is equivalent to a continuity equation for $\rho(\theta, t)$, as follows:

$$\frac{\partial}{\partial t}\rho(\theta,t) + \frac{\partial}{\partial \theta}\{[\bar{\omega}(t) - \lambda \sin(\theta - \alpha)]\rho(\theta,t)\} = 0, \quad (6)$$

where $\bar{\omega}$ is the effective frequency of the system defined by $\bar{\omega}(t) = \omega - \lambda \int_0^{2\pi} \rho(\theta,t)\sin(\theta+\alpha)d\theta$.

Notice that when $\bar{\omega}(t) - \lambda \sin(\theta - \alpha) = 0$ the stationary density $\rho_0(\theta)$ tends to a Dirac function $\rho_0(\theta) = \delta[\theta - \alpha - \arcsin(\bar{\omega}/\lambda)]$. As a result, the effective frequency $\bar{\omega}$ can be obtained self-consistently. After some calculations, it can be easily checked that $\rho_0(\theta)$ corresponds to the HFP discussed above. For the situation of nonzero velocity at each instant of time, the stationary distribution (splay state) becomes

$$\rho_s(\theta) = \pm \frac{\sqrt{\bar{\omega}^2 - \lambda^2}/(2\pi)}{\bar{\omega} - \lambda \sin(\theta - \alpha)}, \quad (7)$$

where the choice of "±" is determined by the sign of $\bar{\omega}$ that makes $\rho_s(\theta)$ positive.

One can further investigate the stability of $\rho_s(\theta)$ against small perturbations. Letting $\rho(\theta,t) = \rho_s(\theta) + \delta\rho(\theta,t)$ and plugging it into Eq. (6), the linearized equation for the evolution of $\delta\rho(\theta,t)$ is obtained as

$$\frac{\partial}{\partial t}\delta\rho(\theta,t) = \widehat{L}(\rho_s)\delta\rho(\theta,t), \quad (8)$$

where $\widehat{L}(\rho_s)$is the operator defined by

$$\widehat{L}(\rho_s)\delta\rho(\theta,t) = \frac{\partial}{\partial\theta}\{[\bar{\omega} - \lambda\sin(\theta-\alpha)]\delta\rho(\theta,t)\} + \frac{\partial\rho_s(\theta)}{\partial\theta}\int_0^{2\pi} d\theta' \lambda \sin(\theta'+\alpha)\delta\rho(\theta',t). \quad (9)$$

In order to diagonalize $\widehat{L}$, one can choose a set of orthogonal bases $\rho_s(\theta)\exp\{2\pi i n G(\theta)\}$, and expand $\delta\rho(\theta,t)$ as

$$\delta\rho(\theta,t) = \sum_{n=-\infty}^{\infty} a_n(t)\rho_s(\theta)\exp\{2\pi i n G(\theta)\}, \quad (10)$$

where $G(\theta) = \int_0^\theta d\theta' \rho_s(\theta')$ is an indefinite integral. If $\rho_s(\theta) = 1/(2\pi)$ the expansion of Eq. (10) is in fact the Fourier decomposition, and [in consideration of the normalization condition for $\rho(\theta,t)$] one has $a_0 \equiv 0$. The continuity equation (8) turns out to be a set of infinite-dimensional ordinary differential equations (all details are discussed in Appendix D):

$$\frac{da_n}{dt} = -2\pi i n C a_n + b_n \sum_{m=-\infty}^{\infty} f_m a_m. \quad (11)$$

A careful examination of Eq. (11) suggests that the matrix of $\widehat{L}$ can be written as $\mathbf{L} = \mathbf{L}_1 \oplus \mathbf{L}_2$, where $\mathbf{L}_1$ is an infinite-dimensional diagonalizable matrix with pure imaginary elements $-2\pi i C l$ ($|l| \neq 1$), and $\mathbf{L}_2$ is a 2×2 submatrix with two eigenvalues. The eigenspectrum structure of $\widehat{L}$ implies then that ρ_s can be stable in at most two nontrivial directions [$\mathrm{Tr}(\mathbf{L}_2) < 0$, $\mathrm{Det}(\mathbf{L}_2) > 0$, Fig. 1], i.e., $\lambda < \omega/(2\cos^2\alpha)$ for $\alpha \in (-\pi/2, -\pi/4)$ and $\lambda < \omega/\sqrt{1+2\cos 2\alpha}$ for $\alpha \in (-\pi/4, 0)$.

Figure 1 illustrates the full phase diagram of Eq. (2) in the space formed by the rescaled parameters α/π and λ/ω. The regions of existence and stability of each steady state are differently colored (see the caption of the figure for all details). Figure 2 reports instead several typical phase transitions along some vertical and horizontal path of Fig. 1, with $\rho_s(\theta)$, which is neutral along most of the perturbation directions. The area where $\rho_s(\theta)$ is neutral is termed as the *marginal* region due to the nontrivial dynamical properties that take place in it [31]. However, a full understanding of the geometric attributes and of the origin of the marginal region in high-dimensional phase spaces is yet not available [31,33].

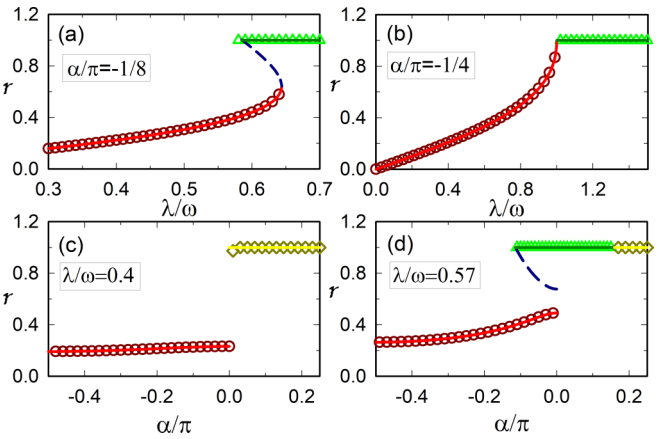

FIG. 2. The order parameter r vs the rescaled parameters λ/ω (first row) and α/π (second row) depicting, respectively, different horizontal and vertical paths in Fig. 1. (a) First-order phase transition occurring from the splay state to HFP (with hysteresis). (b) Continuous phase transition taking place from the splay state to HFP. (c) Discontinuous synchronization transition occurring from the splay state to HLC. (d) Tiered synchronization transition occurring from the splay state to HLC through HFP (with hysteresis). Solid (dashed) lines represent the theoretically predicted stable (unstable) solutions. Red circles denote the splay state, while green triangles (yellow diamonds) stand for HFP (HLC). All symbols refer to numerical simulations performed with a system size $N = 100\,000$.

III. GEOMETRIC IMPLICATIONS OF THE EIGENSPECTRUM

As a next step, we then focus on the macroscopic dynamics [order parameters $z_n = (\sum_{j=1}^N e^{in\theta_j})/N$] in order to capture

the mechanisms behind the stability of the steady states and, in particular, to reveal the origin of the marginal region. Equation (2) can be rewritten as

$$\dot{\theta}_i = f e^{i\theta_i} + g + f^* e^{-i\theta_i}, \tag{12}$$

where $f = i\lambda e^{-i\alpha}/2$, the star denotes the complex conjugate, and $g = \omega - \lambda\,\mathrm{Im}(z_1)\cos\alpha - \lambda\,\mathrm{Re}(z_1)\sin\alpha$. The Ott-Antonsen (OA) ansatz [$z_n = (z_1)^n$] defines an invariable submanifold in the phase space of Eq. (12). When the initial phase distribution takes the form of a Poisson kernel [36,37], Eq. (12) then evolves to

$$\frac{dz_1}{dt} = i\big(f z_1^2 + g z_1 + f^*\big). \tag{13}$$

The HFP is a fixed point of Eq. (13) on the unit circle ($\mathrm{Re}z_{1,h} = \cos\theta_0$, $\mathrm{Im}z_{1,h} = \sin\theta_0$), and the relevant Jacobian matrix has there the same eigenvalues $\delta_{1,2}$ of $\mathbf{J}$ in Eq. (5), with different multiplicities. In such a representation, the eigenvector $\mathbf{V}_1'(\delta_1) = (\cos\alpha,\ -\sin\alpha)^T$ is independent of HFP, and $\mathbf{V}_2'(\delta_2) = (-\mathrm{Im}z_{1,h},\ \mathrm{Re}z_{1,h})^T$ is perpendicular to its radical vector formed by HFP. In fact, $\mathbf{V}_{1(2)}'$ can be viewed as a map of $\mathbf{V}_{1(2)}'$ between the order parameter and the phase descriptions.

Now, a uniform perturbation $\mathbf{V}_2$ ($\delta\theta_j = \epsilon,\ \forall j$) lies along the synchronization manifold: its direction is invariant (after mapping) under a linear approximation and can be written as $\delta z_1 = z_{1,h}(e^{i\epsilon} - 1) \approx \epsilon z_{1,h} e^{i\pi/2}$, which corresponds indeed to $\mathbf{V}_2'$ and is a normal vector to the unit circle at HFP. In contrast, a nonuniform perturbation $\mathbf{V}_1$ ($\sum_{j=1}^N \delta\theta_j = 0$) is perpendicular to the synchronization manifold: the linear approximation fails, however, since $z_{1,h}[(\sum_{j=1}^N e^{i\delta\theta_j})/N - 1] \approx -(z_{1,h}\sum_{j=1}^N \delta\theta_j^2)/(2N)$, and the map of $\mathbf{V}_1$ degenerates to the constant vector $\mathbf{V}_1'$.

The splay state is another fixed point of Eq. (13) inside the unit circle ($\dot{z}_1 = 0$, $|z_1| < 1$), satisfying $\mathrm{Re}z_{1,s}/\mathrm{Im}z_{1,s} = -\tan\alpha$, and the solution $y_\pm = \mathrm{Im}z_{1,s}$ corresponds to $\rho_s(\theta, \bar{\omega}_\mp)$, respectively. After careful calculations, one finds that the eigenvalues of the Jacobian matrix at the splay state are the same as those of $\mathbf{L}_2$. Therefore, one can conclude that the two nontrivial eigenvectors in the marginal region represent essentially the perturbation along the OA manifold, while the presence of the other $N-2$ (purely imaginary) eigenvalues reveals that the OA manifold itself is neutral in the marginal region.

Our analysis suggests that $\alpha = 0$ is a critical scenario. First, it makes the HFP attractive globally, when λ is large enough (see Appendix B for the full details). Second, the orbits of the order parameter $z_1(t)$ are periodic in the OA manifold, and all the perturbations to the splay state can never converge (i.e., $\mathbf{L}_2$ has two pure imaginary eigenvalues) in the marginal region. It is then intriguing to study the nonlinear evolution of the order parameter near the fixed point $[0,\ (\omega - \sqrt{\omega^2 - 3\lambda^2})/(3\lambda)]$ in the center manifold. The orbit of the order parameter (in polar coordinates) is given by (see Appendix E for the derivation)

$$\frac{dr}{d\varphi} = R_2(\varphi) r^2 + R_3(\varphi) r^3. \tag{14}$$

A successive expansion $r(\varphi,\ \epsilon) = r_1(\varphi)\epsilon + r_2(\varphi)\epsilon^2 + \cdots$ is needed to describe the orbit behavior near the center point, and one can prove that the orbits in phase space are strictly closed regardless on the influence of the nonlinear terms. Such closed orbits can be attributed to a quasi-Hamiltonian property that the system features in the absence of phase shift α [30]. One further finds that the dynamical system $\mathfrak{D}$ [Eq. (13)] is invariant under the transformation $\widehat{T}_t\widehat{W}$, where $\widehat{T}_t$ is a time-reversal operator given by $\widehat{T}_t\mathfrak{D}(t) = \mathfrak{D}(-t)$ and $\widehat{W}$ is a space-reversal operator given by $\widehat{W}[\mathrm{Re}z_1(t),\ \mathrm{Im}z_1(t)] = [-\mathrm{Re}z_1(t),\ \mathrm{Im}z_1(t)]$. This symmetry indicates that all the times that an attractor appears on the right half plane ($\mathrm{Re}z_1 > 0$) an opposite repeller must emerge in the symmetric location ($\mathrm{Re}z_1 < 0$). In particular, if the fixed point locates at the y axis, it can be only a saddle or a center. Meanwhile, the condition $\widehat{W}\mathfrak{D} = \widehat{T}_t\mathfrak{D}$ ensures that if an orbit goes across the invariant set (the y axis) twice at different locations then such an orbit must be closed in the phase space.

IV. CONCLUSIONS

In summary, we considered populations of phase oscillators interacting with a starlike configuration. Several different synchronous states (and their dynamical properties) have been identified, and the phase transitions among such collective states have been determined analytically. The relaxation rates, characterizing the time scale of the decay to each stationary state, are crucial parameters. The special eigenspectrum structure for the splay state in the marginal regime is rooted in the characteristic of the OA manifold. Moreover, the quasi-Hamiltonian property which is related to coupling symmetry in the critical case ($\alpha = 0$) is further clarified by considering the nonlinear evolution of the order parameter near the center manifold. Our results are of particular value because almost all biological and technological networked systems in the real world feature disassortative degree-degree correlations, and thus their backbone is essentially made by a collection of leading hubs which interact with surrounding leaves in starlike configurations. Having fully described how SLNs synchronize, this paper paves the way for a better understanding of the functioning of such systems.

ACKNOWLEDGMENTS

This work is partially supported by the National Natural Science Foundation of China (Grants No. 11875135, No. 11875132, No. 11847013, and No. 11835003), the Scientific Research Funds of Huaqiao University (Grants No. 15BS401 and No. 600005-Z17Y0064), the China Scholarship Council scholarship, and the Natural Science Foundation of Shanghai (Grant No. 18ZR1411800).

APPENDIX A: EIGENVALUES OF THE JACOBIAN MATRIX AT HFP

In this Appendix, we give a detailed analysis of the Jacobian matrix $\mathbf{J}$. Substituting $\theta_i(t) = \theta_0 + \delta\theta_i(t)$ into Eq. (1) of the main text (and preserving the leading-order term in $\delta\theta_i$), one obtains

$$\delta\dot{\theta}_i = -\lambda\cos(\theta_0 - \alpha)\delta\theta_i - \frac{\lambda}{N}\sum_{j=1}^{N}\cos(\theta_0 + \alpha)\delta\theta_j. \tag{A1}$$

In matrix form one has $\delta\dot{\theta}_i = \mathbf{J}(\theta_0)\delta\theta_i(t)$. $\mathbf{J}$ is the following $N\times N$ matrix:

$$\mathbf{J} = \begin{pmatrix} a+b & b & \cdots & b \\ b & a+b & \cdots & b \\ \vdots & \vdots & \ddots & \vdots \\ b & b & \cdots & a+b \end{pmatrix}_{N\times N}, \tag{A2}$$

where $a=-\lambda\cos(\theta_0-\alpha)$, $b=-\frac{\lambda}{N}\cos(\theta_0+\alpha)$. According to the fundamental theorem of algebra, $\mathbf{J}$ has only N eigenvalues in the complex plane, and can be further decomposed as

$$\mathbf{J} = \begin{pmatrix} a & & 0 \\ & \ddots & \\ 0 & & a \end{pmatrix}_{N\times N} + \begin{pmatrix} b & b & \cdots & b \\ b & b & \cdots & b \\ \vdots & \vdots & \ddots & \vdots \\ b & b & \cdots & b \end{pmatrix}_{N\times N}. \tag{A3}$$

The first term is a diagonal matrix with equal elements a, and the second is a rank-1 identity matrix. According to the matrix analysis theorem for a normal matrix $\mathbf{A}$ of eigenspectrum

$$\sigma(\mathbf{A}) = \{\delta_1,\ldots,\delta_1,\delta_2,\ldots,\delta_2,\ldots,\delta_p,\ldots,\delta_p\}, \tag{A4}$$

assuming δ_j is k_j-fold degenerate, $j\in\{1,\ldots,p\}$, the multiplicity k_j satisfies

$$\sum_{j=1}^{p} k_j = N. \tag{A5}$$

If a rank-1 matrix $\mathbf{F}$ is added to $\mathbf{A}$, then the eigenspectrum of $\mathbf{A}+\mathbf{F}$ is

$$\sigma(\mathbf{A}+\mathbf{F}) = \{\delta_1,\ldots,\delta_1,\delta_2,\ldots,\delta_2,\delta_p,\ldots,\delta_p,\text{other } p\}, \tag{A6}$$

where δ_j is (k_j-1)-fold degenerate, and $j\in\{1,\ldots,p\}$.

It is clear that the first term in Eq. (A3) is a normal matrix, and the associated eigenvalue is N-fold degenerate. Based on the rank-1 perturbation theory, $\mathbf{J}$ has an eigenvalue $\delta_1 = a$ [$(N-1)$-fold degenerate]. The other eigenvalue δ_2 (single degenerate) can be calculated by the property

$$(N-1)\delta_1 + \delta_2 = \mathrm{Tr}(\mathbf{J}), \tag{A7}$$

which yields $\delta_2 = a+Nb$.

APPENDIX B: THE STABILITY OF THE PHASE-LOCKED STATES AT $\alpha = 0$

In this Appendix, we will prove that all the phase-locked states are unstable when $\alpha = 0$. Let $z_1 = re^{i\Psi}$, then Eq. (1) of the main text can be rewritten in its mean-field form:

$$\dot{\theta}_i = \omega - \lambda r\sin\Psi - \lambda\sin\theta_i, \quad i = 1,\ldots,N. \tag{B1}$$

The fixed points of Eq. (B1) correspond to $\dot{\theta}_i = 0$, which yields

$$\sin\theta_i = \frac{\omega}{\lambda} - r\sin\Psi. \tag{B2}$$

Summing both sides of Eq. (B2) and using the definition of z_1, one has

$$r\sin\Psi = \frac{\omega}{2\lambda}. \tag{B3}$$

Then, the existence condition of phase-locked states is $\lambda \geqslant \omega/2$. Substituting Eq. (B3) into Eq. (B2), one obtains $\sin\theta_i = \omega/(2\lambda)$ and

$$\cos\theta_i = h(i)\sqrt{1-\frac{\omega^2}{4\lambda^2}}, \quad i = 1,\ldots,N, \tag{B4}$$

where $h(i) = \pm 1$ if all $h(i)$ have the same sign (i.e., for the state called HFP in the main text), while the other $N-1$ cases correspond to phase-locked states with $|z_1| < 1$. Similarly, the Jacobian matrix at these phase-locked states is

$$\mathbf{J} = -\frac{\lambda}{N}\sqrt{1-\frac{\omega^2}{4\lambda^2}} \times \begin{pmatrix} (N+1)h(1) & h(2) & \cdots & h(N) \\ h(1) & (N+1)h(2) & \cdots & h(N) \\ \vdots & \vdots & \ddots & \vdots \\ h(1) & h(2) & \cdots & (N+1)h(N) \end{pmatrix}. \tag{B5}$$

According to rank-1 perturbation theory, if all $h(i)$ are the same, the $(N-1)$ multiple eigenvalue is $\delta_1 = -\lambda h(i)\sqrt{1-\omega^2/(4\lambda^2)}$, and $\delta_2 = -2\lambda h(i)\sqrt{1-\omega^2/(4\lambda^2)}$. Clearly, HFP is unstable for $h(i) = -1$.

Let now $h(i) = 1$, $i = 1,\ldots,m$ and $h(i) = -1$, $i = m+1,\ldots,N$. Then, two kinds of eigenvalues in $\mathbf{J}$ can be obtained directly from rank-1 perturbation theory: the first one is a $(m-1)$ multiple root $\mu_1 = -\lambda\sqrt{1-\omega^2/(4\lambda^2)}$, and the second one $\mu_2 = \lambda\sqrt{1-\omega^2/(4\lambda^2)}$ is a $(N-m-1)$ multiple root that is always positive. Therefore, all the phase-locked states (except HFP) are unstable.

APPENDIX C: STABILITY OF THE N_c-CLUSTER STATE

As mentioned in the main text, HFP and HLC are the simplest solutions of the system. Actually, there may exist a class of slightly complicated collective behaviors, namely, the N_c-cluster state, where the system evolves to a N_c-dimensional invariant torus:

$$\dot{\Phi}_k = \omega - \lambda\sin(\Phi_k-\alpha) - \lambda\sum_{j=1}^{N_c}\epsilon_j\sin(\Phi_j+\alpha), \quad k = 1,\ldots,N_c. \tag{C1}$$

Here ϵ_j is the ratio of the jth cluster and satisfies the normalization condition

$$\sum_{j=1}^{N_c}\epsilon_j = 1. \tag{C2}$$

Linear stability analysis of the N_c-cluster state shows that the Jacobian matrix $\mathbf{J}$ is a $N\times N$ block matrix, where the kth diagonal $(\mathbf{M})_{kk}$ is a cyclic matrix:

$$(\mathbf{M})_{kk} = \begin{pmatrix} a_k & b_k & \cdots & b_k \\ b_k & a_k & \cdots & b_k \\ \vdots & \vdots & \ddots & \vdots \\ b_k & b_k & \cdots & a_k \end{pmatrix}_{\epsilon_k N\times\epsilon_k N}, \tag{C3}$$

with diagonal elements a_k and the off-diagonal elements b_k. The other off-diagonal block $(\mathbf{M})_{kl}$ is

$$(\mathbf{M})_{kl} = -\lambda\cos(\Phi_l+\alpha)\begin{pmatrix}1 & 1 & \cdots & 1\\ 1 & 1 & \cdots & 1\\ \vdots & \vdots & \ddots & \vdots\\ 1 & 1 & \cdots & 1\end{pmatrix}_{\epsilon_k N\times\epsilon_k N}. \tag{C4}$$

The mth element of the n_kth eigenvector of $(\mathbf{M})_{kk}$ is

$$(V_m)_{n_k} = \exp\left\{\frac{2\pi i n_k m}{\epsilon_k N}\right\}, \tag{C5}$$

where $n_k \in \{0, 1, \ldots, \epsilon_k N-1\}$, $m \in \{1, \ldots, \epsilon_k N\}$.

The eigenvalue associated to $\mathbf{V}_{n_k}$ reads

$$\delta_{n_k} = -\lambda\cos(\Phi_k-\alpha), \quad 1 \leqslant n_k \leqslant \epsilon_k N-1, \tag{C6}$$

$$\delta_0 = -2\lambda\cos\alpha\cos\Phi_k, \quad n_k = 0. \tag{C7}$$

One then constructs the eigenvector $\mathbf{V}$ of $\mathbf{J}$ as

$$\mathbf{V} = (0, \ldots, \mathbf{V}_{nk}, 0, \ldots, 0)^T. \tag{C8}$$

It can be easily verified that the relevant eigenvalue is δ_{n_k} ($n_k \neq 0$). Hence, the N_c necessary conditions for the stability of the N_c-cluster state are $I_k < 0, k = 1, \ldots, n_k$, which reads

$$\begin{aligned} I_k &= -\int_0^{t_p} dt\lambda\cos[\Phi_k(t)-\alpha]\\ &= -\int_0^{2\pi} d\Phi_k\lambda\cos(\Phi_k-\alpha)\frac{1}{\dot{\Phi}_k}\\ &= -\int_0^{2\pi}\frac{\lambda\cos(\Phi_k-\alpha)d\Phi_k}{\omega-\lambda\sin(\Phi_k-\alpha)-\lambda\sum_{j=1}^{N_c}\epsilon_j\sin(\Phi_j+\alpha)}. \end{aligned} \tag{C9}$$

It is difficult to get explicit stability criteria for generic directional perturbations. However, when $N_c = 1$, the system degenerates to HLC and one gets

$$\begin{aligned} I_1 &= \int_0^{T_p} dt\delta_1(t)\\ &= -\int_0^{T_p} dt\lambda\cos[\theta(t)-\alpha]\\ &= -\int_0^{2\pi} d\theta\lambda\cos(\theta-\alpha)\frac{dt}{d\theta}\\ &= -\int_0^{2\pi} d\theta\frac{\lambda\cos(\theta-\alpha)}{\omega-2\lambda\cos\alpha\sin\theta}\\ &= -\pi\tan\alpha\left[-1+\frac{\omega}{\sqrt{\omega^2-(2\lambda\cos\alpha)^2}}\right], \end{aligned} \tag{C10}$$

and

$$\begin{aligned} I_2 &= \int_0^{T_p} dt\delta_2(t)\\ &= -2\lambda\cos\alpha\int_0^{T_p} dt\cos[\theta(t)]\\ &= -2\lambda\cos\alpha\int_0^{2\pi} d\theta\cos\theta\frac{d\theta}{dt}\\ &= -2\lambda\cos\alpha\int_0^{2\pi} d\theta\frac{\cos\theta}{\omega-2\lambda\cos\alpha\sin\theta} \equiv 0. \end{aligned} \tag{C11}$$

APPENDIX D: STABILITY OF THE STATIONARY DISTRIBUTION

According to Eq. (3) of the main text, when the velocity $\bar{\omega}-\lambda\sin(\theta-\alpha) = 0$, the distribution $\rho(\theta,t)$ becomes stationary. Then the effective frequency $\bar{\omega}$ is

$$\begin{aligned} \bar{\omega} &= \omega-\lambda\int_0^{2\pi}\delta\left(\theta-\alpha-\arcsin\frac{\bar{\omega}}{\lambda}\right)\sin(\theta+\alpha)d\theta\\ &= \omega-\lambda\sin\left(2\alpha+\arcsin\frac{\bar{\omega}}{\lambda}\right). \end{aligned} \tag{D1}$$

Solving it, one obtains

$$\bar{\omega} = \frac{\lambda}{4}\sec^2\alpha\left[\frac{\omega}{\lambda}\cos^2\alpha\pm\sqrt{\left(4\cos^2\alpha-\frac{\omega^2}{\lambda^2}\right)\sin^2 2\alpha}\right]. \tag{D2}$$

Substituting it into $\rho_0(\theta)$, one has

$$\begin{aligned} \sin\theta &= \sin\left(\alpha+\arcsin\frac{\bar{\omega}}{\lambda}\right)\\ &= \frac{\omega}{2\lambda\cos\alpha}, \end{aligned} \tag{D3}$$

which corresponds to HFP. When the velocity $v_\theta \neq 0$, the stationary distribution is a smooth function $\rho_s(\theta)$ [Eq. (4) of the main text], and one has

$$\begin{aligned} \langle\sin\theta\rangle &= \int_0^{2\pi}\sin\theta\rho_s(\theta)d\theta\\ &= \pm\frac{\sqrt{\bar{\omega}^2-\lambda^2}}{2\pi}\int_0^{2\pi}\frac{\sin(\theta+\alpha)}{\bar{\omega}-\lambda\sin\theta}d\theta\\ &= \cos\alpha\frac{\bar{\omega}}{\lambda}\left(1-\sqrt{1-\frac{\lambda^2}{\bar{\omega}^2}}\right), \end{aligned} \tag{D4}$$

and

$$\begin{aligned} \langle\cos\theta\rangle &= \int_0^{2\pi}\cos\theta\rho_s(\theta)d\theta\\ &= \pm\frac{\sqrt{\bar{\omega}^2-\lambda^2}}{2\pi}\int_0^{2\pi}\frac{\cos(\theta+\alpha)}{\bar{\omega}-\lambda\sin\theta}d\theta\\ &= -\sin(\alpha)\frac{\bar{\omega}}{\lambda}\left(1-\sqrt{1-\frac{\lambda^2}{\bar{\omega}^2}}\right). \end{aligned} \tag{D5}$$

Then, the effective frequency $\bar{\omega}$ becomes

$$\begin{aligned} \bar{\omega} &= \omega-\lambda(\langle\sin\theta\rangle\cos\alpha+\langle\cos\theta\rangle\sin\alpha)\\ &= \omega-\bar{\omega}\left(1-\sqrt{1-\frac{\lambda^2}{\bar{\omega}^2}}\right)\cos 2\alpha. \end{aligned} \tag{D6}$$

Solving it, one obtains

$$\bar{\omega}_\pm = \frac{\omega(1+\cos 2\alpha)\pm\cos 2\alpha\sqrt{\omega^2-\lambda^2(1+2\cos 2\alpha)}}{1+2\cos 2\alpha}. \tag{D7}$$

The existence region of $\bar{\omega}$ must ensure that the radical expressions in Eqs. (D6) and (D7) are real. Then, the area for $\rho_s(\theta, \bar{\omega} > \lambda)$ is

$$\lambda > 0, \quad |\alpha| \in \left(\frac{\pi}{3}, \frac{\pi}{2}\right), \tag{D8}$$

$$\lambda \in \left(0, \frac{\omega}{\sqrt{1+2\cos 2\alpha}}\right), \quad |\alpha| < \frac{\pi}{3}, \tag{D9}$$

and the area for $\rho_s(\theta, \bar{\omega} < -\lambda)$ is

$$\lambda \in \left[0, \frac{\omega}{2\cos^2\alpha}\right], \quad \alpha \in \left(-\frac{\pi}{2}, \frac{\pi}{2}\right), \tag{D10}$$

$$\lambda \in \left(\frac{\omega}{2\cos^2\alpha}, \frac{\omega}{\sqrt{1+2\cos 2\alpha}}\right), \quad |\alpha| \in \left(\frac{\pi}{4}, \frac{\pi}{2}\right). \tag{D11}$$

Substituting Eq. (8) into Eq. (6), one obtains

$$b_n = \int_0^{2\pi} d\theta \frac{d\rho_s}{d\theta} e^{-2\pi i n G(\theta)}, \tag{D12}$$

$$f_m = \int_0^{2\pi} d\theta \lambda \sin(\theta+\alpha)\rho_s(\theta) e^{2\pi i m G(\theta)}. \tag{D13}$$

It is now convenient to change the integral variable θ into G, and to set $\theta' = \theta - \alpha$. The result is

$$\frac{d\theta'}{dt} = \bar{\omega} - \lambda \sin\theta'. \tag{D14}$$

The indefinite integral $G(\theta')$ associated with $\rho_s(\theta')$ is

$$G(\theta') = \int_0^{\theta'} d\theta'' \rho_s(\theta''), \tag{D15}$$

and one has

$$\frac{d\theta'}{dG} = \frac{\bar{\omega}}{C} - \frac{\lambda}{C}\sin\theta', \tag{D16}$$

which is a typical overdamped pendulum equation, and $C = \sqrt{\bar{\omega}^2 - \lambda^2}/(2\pi)$. If $\bar{\omega} > \lambda$, the solution of Eq. (D16) is

$$\theta'(G) = 2\arctan\left(\frac{2\pi C}{\bar{\omega}}\tan\pi(G - G_1) + \frac{\lambda}{\bar{\omega}}\right). \tag{D17}$$

Using the initial condition $\theta'(0) = 0$, one gets

$$\tan\pi G_1 = \frac{\lambda}{\sqrt{\bar{\omega}^2 - \lambda^2}}. \tag{D18}$$

Considering that $\sin[\theta'(G)] = 2\tan(\theta'/2)/[1+\tan^2(\theta'/2)]$, and multiplying the numerator and the denominator by $\cos^2\pi(G - G_1)$, one has

$$\sin[\theta'(G)] = \frac{\lambda + \bar{\omega}\sin 2\pi(G - \bar{G})}{\bar{\omega} + \lambda\sin 2\pi(G - \bar{G})}. \tag{D19}$$

Similarly, taking into consideration that $\cos\theta' = [1 - \tan^2(\theta'/2)]/[1+\tan^2(\theta'/2)]$, one gets

$$\cos[\theta'(G)] = \frac{\sqrt{\bar{\omega}^2 - \lambda^2}\cos 2\pi(G - \bar{G})}{\bar{\omega} + \lambda\sin 2\pi(G - \bar{G})}. \tag{D20}$$

Substituting Eqs. (D19) and (D20) into Eq. (D12), one obtains

$$\begin{aligned} b_n &= 2\pi i n \int_0^1 dG \frac{C}{\bar{\omega} - \lambda\sin\theta'} e^{-2\pi i n G} \\ &= \frac{n\lambda}{2\sqrt{\bar{\omega}^2 - \lambda^2}}\left(e^{-2\pi i \bar{G}}\delta_{n,1} - e^{2\pi i \bar{G}}\delta_{n,-1}\right), \end{aligned} \tag{D21}$$

where $\bar{G} = \frac{1}{2\pi}\arctan\frac{\lambda}{\sqrt{\bar{\omega}^2-\lambda^2}}$.

Next, the expansion of f_m is given by

$$\begin{aligned} f_m &= \int_0^{2\pi} d\theta' \lambda \sin(\theta' + 2\alpha)\rho_s(\theta') e^{2\pi i m G} \\ &= \int_0^1 dG \frac{d\theta'}{dG}\lambda\sin(\theta' + 2\alpha)\rho_s(\theta') e^{2\pi i m G} \\ &= \int_0^1 dG \lambda(\sin\theta'\cos 2\alpha + \cos\theta'\sin 2\alpha) e^{2\pi i m G}, \end{aligned} \tag{D22}$$

where

$$\begin{aligned} &\int_0^1 dG \sin\theta' e^{2\pi i m G w} \\ &= e^{2\pi i m G}\int_0^1 dG \frac{\lambda + \bar{\omega}\sin 2\pi G}{\bar{\omega} + \lambda\sin 2\pi G} e^{2\pi i m G} \\ &= \frac{1}{2\pi} e^{2\pi i m \bar{G}} \int_0^{2\pi} d\theta \frac{\lambda + \bar{\omega}\sin\theta}{\bar{\omega} + \lambda\sin\theta} e^{im\theta} \\ &= \frac{1}{2\pi} e^{2\pi i m \bar{G}} \left\{ \lambda \int_0^{2\pi} d\theta \frac{e^{im\theta}}{\bar{\omega} + \lambda\sin\theta} \right. \\ &\quad + \frac{\bar{\omega}}{2i}\int_0^{2\pi} d\theta \frac{e^{i(m+1)\theta}}{\bar{\omega} + \lambda\sin\theta} - \left.\frac{\bar{\omega}}{2i}\int_0^{2\pi} d\theta \frac{e^{i(m-1)\theta}}{\bar{\omega} + \lambda\sin\theta}\right\}. \end{aligned} \tag{D23}$$

Based on the theorem of the residue, when $\bar{\omega} > \lambda$ one obtains

$$\begin{aligned} f_m = \lambda e^{2\pi i m \bar{G}} i^{m-1} &\frac{(\bar{\omega} - \sqrt{\bar{\omega}^2 - \lambda^2})^m}{(-\lambda)^{m+1}} \\ &\times \sqrt{\bar{\omega}^2 - \lambda^2}(\sin 2\alpha + i\cos 2\alpha), \end{aligned} \tag{D24}$$

while when $\bar{\omega} < \lambda$ one gets

$$\begin{aligned} f_m = \lambda e^{2\pi i m \bar{G}} i^{m-1} &\frac{(\bar{\omega} + \sqrt{\bar{\omega}^2 - \lambda^2})^m}{(-\lambda)^{m+1}} \\ &\times \sqrt{\bar{\omega}^2 - \lambda^2}(\sin 2\alpha - i\cos 2\alpha). \end{aligned} \tag{D25}$$

APPENDIX E: NONLINEAR EVOLUTION OF THE SYSTEM IN THE MARGINAL REGION

When $\alpha = 0$, Eq. (10) of the main text has two fixed points $(x,\ y_\pm)$, where $x = 0$ and $y_\pm = (\omega \pm \sqrt{\omega^2 - 3\lambda^2})/(2\lambda)$. Linear stability analysis shows that $(x,\ y_+)$ is a saddle and $(x,\ y_-)$ is a center. To study the characteristic of this fixed point, one further considers the effects generated by nonlinear terms near the center $(x,\ y_-)$. Translating the coordinate $(x,\ y_-)$ into $(0,\ 0)$, Eq. (10) of the main text becomes

$$\dot{x} = -a_1 y + a_2 y^2 - a_3 x^2, \tag{E1}$$

$$\dot{y} = b_1 x - b_2 xy, \tag{E2}$$

in the Cartesian coordinates, where $a_1 = \sqrt{\omega^2 - 3\lambda^2}$, $a_2 = 3/2$, $a_3 = 1/2$, $b_1 = (5\omega - 2\sqrt{\omega^2 - 3\lambda^2})/3$, and $b_2 = 2\lambda$. Scaling the variables $x' = x$ and $y' = \sqrt{a_1/b_1}y$, one obtains the standard form

$$\dot{x} = -by + ay^2 - cx^2, \tag{E3}$$

$$\dot{y} = bx - dxy, \tag{E4}$$

where $a = a_2 b_1/a_1$, $b = \sqrt{a_1 b_1}$, $c = a_3$, and $d = b_2$. In polar coordinates, $x = r\cos\varphi$ and $y = r\sin\varphi$, one gets

$$\frac{dr}{d\varphi} = \frac{r^2}{b}\frac{(a-d)\cos\varphi\sin^2\varphi - c\cos^3\varphi}{1 + r[(c-d)\cos^2\varphi\sin\varphi - a\sin^3\varphi]/b}. \quad \text{(E5)}$$

Expanding Eq. (E5) near $r = 0$, one has

$$\frac{dr}{d\varphi} = R_2(\varphi)r^2 + R_3(\varphi)r^3, \quad \text{(E6)}$$

where $R_2(\varphi) = [-c\cos^3\varphi + (a-d)\cos\varphi\sin^2\varphi]/b$ and $R_3(\varphi) = [(d-c)\cos^2\varphi\sin\varphi + a\sin^3\varphi][-c\cos^3\varphi + (a-d)\cos\varphi\sin^2\varphi]/b^2$. Choosing an orbit with initial condition $r = \epsilon$ at $\varphi = 0$, and expanding it with respect to ϵ, one obtains

$$r(\varphi, \epsilon) = r_1(\varphi)\epsilon + r_2(\varphi)\epsilon^2 + \cdots. \quad \text{(E7)}$$

Substituting Eq. (E7) into Eq. (E6), one finally gets the coefficient balance equations associated with $O(\epsilon^n)$ as

$$\frac{dr_1(\varphi)}{d\varphi} = 0, \quad \text{(E8)}$$

$$\frac{dr_2(\varphi)}{d\varphi} = R_2(\varphi)r_1^2(\varphi), \quad \text{(E9)}$$

$$\frac{dr_3(\varphi)}{d\varphi} = R_3(\varphi)r_1^3(\varphi) + 2R_3(\varphi)r_1(\varphi)r_2(\varphi). \quad \text{(E10)}$$

Due to the initial condition $r_1(0) = 1$, $r_2(0) = r_3(0) = \cdots = 0$, it can be seen that $r_i(\varphi)$ is a function of $\sin\varphi$ or $\cos\varphi$, and therefore the orbit is invariant after 2π:

$$r(\varphi + 2\pi, \epsilon) = r(\varphi, \epsilon). \quad \text{(E11)}$$

Since ϵ is arbitrary, the conclusion is that all orbits near the center point are closed.

[1] A. Pikovsky, M. Rosenblum, and J. Kurths, *Synchronization: A Universal Concept in Nonlinear Sciences* (Cambridge University Press, Cambridge, England, 2001); S. Boccaletti, A. N. Pisarchik, C. I. del Genio, and A. Amann, *Synchronization: From Coupled Systems to Complex Networks* (Cambridge University Press, Cambridge, England, 2018).

[2] S. H. Strogatz, *Sync: The Emerging Science of Spontaneous Order* (Hachette Books, New York, 2003).

[3] M. Rohden, A. Sorge, M. Timme, and D. Witthaut, Phys. Rev. Lett. **109**, 064101 (2012).

[4] I. Z. Kiss, Y. Zhai, and J. L. Hudson, Science **296**, 1676 (2002).

[5] B. Georges, J. Grollier, V. Cros, and A. Fert, Appl. Phys. Lett. **92**, 232504 (2008).

[6] G. Buzsáki and A. Draguhn, Science **304**, 1926 (2004).

[7] A. T. Winfree, J. Theor. Biol. **16**, 15 (1967).

[8] B. Eckhardt, E. Ott, S. H. Strogatz, D. M. Abrams, and A. McRobie, Phys. Rev. E **75**, 021110 (2007).

[9] J. A. Acebrón, L. L. Bonilla, C. J. P. Vicente, F. Ritort, and R. Spigler, Rev. Mod. Phys. **77**, 137 (2005).

[10] *Lecture Notes in Physics*, edited by Y. Kuramoto (Springer, New York, 1975), Vol. 39.

[11] S. N. Dorogovtsev, A. V. Goltsev, and J. F. F. Mendes, Rev. Mod. Phys. **80**, 1275 (2008).

[12] S. Boccaletti *et al.*, Phys. Rep. **424**, 175 (2006); **544**, 1 (2014); **660**, 1 (2016).

[13] M. Piraveenan, M. Prokopenko, and A. Y. Zomaya, Europhys. Lett. **84**, 28002 (2008).

[14] I. Sendina-Nadal, M. M. Danziger, Z. Wang, S. Havlin, and S. Boccaletti, Sci. Rep. **6**, 21297 (2016).

[15] Y. Kazanovich and R. Borisyuk, Prog. Theor. Phys. **110**, 1047 (2003).

[16] O. Burylko, Y. Kazanovich, and R. Borisyuk, Physica D **241**, 1072 (2012).

[17] Y. Kazanovich *et al.*, Physica D **261**, 114 (2013).

[18] V. Vlasov, E. E. N. Macau, and A. Pikovsky, Chaos **24**, 023120 (2014).

[19] V. Vlasov, A. Pikovsky, and E. E. N. Macau, Chaos **25**, 123120 (2015).

[20] J. A. Kromer, L. Schimansky-Geier, and A. B. Neiman, Phys. Rev. E **93**, 042406 (2016).

[21] O. Burylko, Y. Kazanovich, and R. Borisyuk, Sci. Rep. **8**, 416 (2018).

[22] K. Y. Tsang, R. E. Mirollo, S. H. Strogatz, and K. Wiesenfeld, Physica D **48**, 102 (1991).

[23] C. Zhou, L. Zemanova, G. Zamora, C. C. Hilgetag, and J. Kurths, Phys. Rev. Lett. **97**, 238103 (2006).

[24] J. Gómez-Gardeñes, S. Gómez, A. Arenas, and Y. Moreno, Phys. Rev. Lett. **106**, 128701 (2011); I. Leyva *et al.*, *ibid.* **108**, 168702 (2012).

[25] Y. Zou, T. Pereira, M. Small, Z. Liu, and J. Kurths, Phys. Rev. Lett. **112**, 114102 (2014).

[26] C. Xu, J. Gao, Y. Sun, X. Huang, and Z. Zheng, Sci. Rep. **5**, 12039 (2015).

[27] V. Vlasov, Y. Zou, and T. Pereira, Phys. Rev. E **92**, 012904 (2015).

[28] P. Kundu, P. Khanra, C. Hens, and P. Pal, Phys. Rev. E **96**, 052216 (2017).

[29] S. Watanabe and S. H. Strogatz, Physica D **74**, 197 (1994).

[30] S. A. Marvel and S. H. Strogatz, Chaos **19**, 013132 (2009).

[31] D. Golomb, D. Hansel, B. Shraiman, and H. Sompolinsky, Phys. Rev. A **45**, 3516 (1992).

[32] S. Watanabe and S. H. Strogatz, Phys. Rev. Lett. **70**, 2391 (1993).

[33] S. H. Strogatz and R. E. Mirollo, Phys. Rev. E **47**, 220 (1993).

[34] R. Zillmer, R. Livi, A. Politi, and A. Torcini, Phys. Rev. E **76**, 046102 (2007).

[35] M. Calamai, A. Politi, and A. Torcini, Phys. Rev. E **80**, 036209 (2009).

[36] E. Ott and T. M. Antonsen, Chaos **18**, 037113 (2008).

[37] E. Ott and T. M. Antonsen, Chaos **19**, 023117 (2009).